ORIGINAL

István Ecsedi · Attila Baksa

Analytical solution for torsion of cylindrical orthotropic annular wedge-shaped bars reinforced by thin shells

Abstract This paper deals with the Saint-Venant torsion of elastic, cylindrically orthotropic bar whose cross section is a sector of a circular ring shaped bar. The cylindrically orthotropic homogeneous elastic wedge-shaped bar strengthened by on its curved boundary surfaces by thin isotropic elastic shells. An analytical method is presented to obtain the Prandtl's stress function, torsion function, torsional rigidity and shearing stresses. A numerical example illustrates the application of the developed analytical method.

Keywords Saint-Venant torsion · Cylindrical orthotropic · Wedge-shape bar · Elastic shell · Prandtl's stress function · Torsion function · Torsional rigidity

1 Introduction

The Saint-Venant torsion of anisotropic linearly elastic bars has been the subject of several works from both theoretical and numerical viewpoints. Books by Lekhnitskii [5,6], Milne-Thomson [8], Arutjujan and Abramjan [1], Sokolnikoff [13], Sadd [10], Sarkisyan [11,12], Rand and Rovenski [9], Chabanjan [2] give the detailed analysis of Saint-Venant torsion of anisotropic and orthotropic bars. The books mentioned above deal with mainly the Saint-Venant torsion of Cartesian anisotropic and orthotropic bars. The torsion problem of cylindrically anisotropic and orthotropic bars is studied in books by Lekhnitskii [5,6], Rand and Rovenski [9] and papers by Soós [14] and Ecsedi et al [4]. In paper [3], by the use of principle of minimum of potential energy and principle of minimum of complementary energy, approximate analytical solutions are derived for the torsion function and for the Prandtl's stress function of the uniform torsion of cylindrically orthotropic solid elliptical cross section.

Present paper deals with the Saint-Venant torsion of cylindrically orthotropic bar whose cross section is a sector of hollow circle. The considered cylindrically orthotropic homogeneous elastic annular wedge-shaped bar strengthened on its curved boundary parts by thin isotropic elastic shells. An analytical solution is formulated to solve the Saint-Venant's torsion problem for the cylindrically orthotropic bar which is reinforced by thin isotropic elastic shells on its curved boundary surfaces. The developed solution gives the Prandtl's stress function, torsion function and the torsional rigidity of the compound cross section which consists of one solid cross section and two open thin walled cross section.

2 Governing equations

At first, we consider the Saint-Venant torsion of the compound linear elastic bar which is constructed from three cylindrical orthotropic beam components whose cross section is shown in Fig. 1.

I. Ecsedi · A. Baksa (✉)
Institute of Applied Mechanics, University of Miskolc, Miskolc-Egyetemváros, Hungary
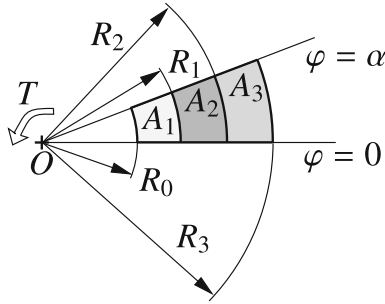E-mail: attila.baksa@uni-miskolc.hu

Fig. 1 Cylindrically orthotropic compound cross section

The cylindrical coordinate system $Or\varphi z$ has been used to formulate the governing equations of the uniform torsion problem of compound annular wedge-shape bar. The cross section A can be divided into three parts as $A = A_1 \cup A_2 \cup A_3$, where

$$A_1 = \{(r, \varphi) | R_0 \leq r \leq R_1, \ 0 \leq \varphi \leq \alpha\} \tag{1}$$

$$A_2 = \{(r, \varphi) | R_1 \leq r \leq R_2, \ 0 \leq \varphi \leq \alpha\} \tag{2}$$

$$A_3 = \{(r, \varphi) | R_2 \leq r \leq R_3, \ 0 \leq \varphi \leq \alpha\} \tag{3}$$

There are perfect connections between the beam components whose cross sections are A_1, A_2 and A_3. From this fact it follows that axial displacement and radial shearing stress field are continuous on the whole cross section A. The length of the compound bar is denoted by L. The material of the beam component $B_i = A_i \times (0, L)$ ($i = 1, 2, 3$) is cylindrically orthotropic with shear modulus G_{ir}, $G_{i\varphi}$ ($i = 1, 2, 3$). In the present problem the Prandtl's stress function formulation of the considered Saint-Venant torsion leads to the next coupled boundary-value problem [2,4–6,9,11,12]

$$\frac{\partial^2 U_1}{\partial r^2} + \frac{1}{r}\frac{\partial U_1}{\partial r} + \frac{g_1^2}{r^2}\frac{\partial^2 U_1}{\partial \varphi^2} = -2G_{1\varphi} \qquad g_1 = \sqrt{\frac{G_{1\varphi}}{G_{1r}}} \quad \text{in } A_1 \tag{4}$$

$$U_1 = 0 \quad R_0 \leq r \leq R_1 \quad \varphi = 0 \quad \text{and} \quad \varphi = \alpha \tag{5}$$

$$\frac{\partial^2 U_2}{\partial r^2} + \frac{1}{r}\frac{\partial U_2}{\partial r} + \frac{g_2^2}{r^2}\frac{\partial^2 U_2}{\partial \varphi^2} = -2G_{2\varphi} \qquad g_2 = \sqrt{\frac{G_{2\varphi}}{G_{2r}}} \quad \text{in } A_2 \tag{6}$$

$$U_2 = 0 \quad R_1 \leq r \leq R_2 \quad \varphi = 0 \quad \text{and} \quad \varphi = \alpha \tag{7}$$

$$\frac{\partial^2 U_3}{\partial r^2} + \frac{1}{r}\frac{\partial U_3}{\partial r} + \frac{g_3^2}{r^2}\frac{\partial^2 U_3}{\partial \varphi^2} = -2G_{3\varphi} \qquad g_3 = \sqrt{\frac{G_{3\varphi}}{G_{3r}}} \quad \text{in } A_3 \tag{8}$$

$$U_3 = 0 \quad R_2 \leq r \leq R_3 \quad \varphi = 0 \quad \text{and} \quad \varphi = \alpha \tag{9}$$

$$U_1(R_0, \varphi) = 0 \qquad 0 \leq \varphi \leq \alpha \tag{10}$$

$$U_3(R_3, \varphi) = 0 \qquad 0 \leq \varphi \leq \alpha \tag{11}$$

$$U_1(R_1, \varphi) = U_2(R_1, \varphi) \qquad 0 \leq \varphi \leq \alpha \tag{12}$$

$$U_2(R_2, \varphi) = U_3(R_2, \varphi) \qquad 0 \leq \varphi \leq \alpha \tag{13}$$

$$\frac{1}{G_{1\varphi}}\frac{\partial U_1}{\partial r} = \frac{1}{G_{2\varphi}}\frac{\partial U_2}{\partial r} \qquad r = R_1 \qquad 0 \leq \varphi \leq \alpha \tag{14}$$

$$\frac{1}{G_{2\varphi}}\frac{\partial U_2}{\partial r} = \frac{1}{G_{3\varphi}}\frac{\partial U_3}{\partial r} \qquad r = R_2 \qquad 0 \leq \varphi \leq \alpha \tag{15}$$

Equations (4), (6) and (8) formulate the strain compatibility conditions in terms of stress function $U_i = U_i(r, \varphi)$ ($i = 1, 2, 3$). The boundary conditions (5), (7), (9), (10) and (11) express that the whole boundary contour of cross section A is traction free. The continuity conditions of radial shearing stresses on the common boundary curve of A_1 and A_2 on the common boundary curve of A_2 and A_3 are formulated by Eqs. (12) and (13). Equations (14) and (15) provide the continuity of the axial displacement over the whole cross section

A. The relation between the Prandtl's stress functions $U_i = U_i(r, \varphi)$ and torsion function $\omega_i = \omega_i(r, \varphi)$ are described by the following systems of equations [2,5,6,9,11,12]

$$G_{ir} \frac{\partial \omega_i}{\partial r} = \frac{1}{r} \frac{\partial U_i}{\partial \varphi}, \quad G_{i\varphi} \frac{\partial \omega_i}{\partial \varphi} = -r \frac{\partial U_i}{\partial r} - G_{i\varphi} r^2 \quad (r, \varphi) \in A_i \quad (i = 1, 2, 3) \tag{16}$$

Equation (16) is based on formulae of shearing stresses $\tau_{irz} = \tau_{irz}(r, \varphi)$ and $\tau_{i\varphi z} = \tau_{i\varphi z}(r, \varphi)$ expressed in terms of $U_i = U_i(r, \varphi)$ and $\omega_i = \omega_i(r, \varphi)$ $(i = 1, 2, 3)$ which are as follows

$$\frac{\tau_{irz}}{\vartheta} = G_{ir} \frac{\partial \omega_i}{\partial r} = \frac{1}{r} \frac{\partial U_i}{\partial \varphi} \quad (i = 1, 2, 3) \tag{17}$$

$$\frac{\tau_{i\varphi z}}{\vartheta} = G_{i\varphi} \left(\frac{1}{r} \frac{\partial \omega_i}{\partial \varphi} + r \right) = -\frac{\partial U_i}{\partial r} \quad (i = 1, 2, 3) \tag{18}$$

In Eqs. (14), (15) ϑ denotes the rate of twist with respect to the axial coordinate z [5,6,8]. The relation between the applied torque T and ϑ is as follows

$$T = \vartheta S \tag{19}$$

where S is the torsional rigidity of the compound cross section A. According to Prandtl's formulation of uniform torsion we have [5,6,11,12]

$$S = 2 \left(\int_{A_1} U_1 \, dA + \int_{A_2} U_2 \, dA + \int_{A_3} U_3 \, dA \right). \tag{20}$$

Here, we note for isotropic beam component the shear modulus in radial and circumferential direction is the same, that is

$$G_r = G_\varphi = G \tag{21}$$

3 Cross section reinforced by thin elastic shells

Figure 2 shows the elastic cylindrically orthotropic cross section which is reinforced by thin isotropic elastic shells on its curved boundary. In the present problem

$$A_1 = \{(r, \varphi) | R_0 \leq r \leq R_1 = R_0 + t_1 \quad 0 \leq \varphi \leq \alpha\} \tag{22}$$

$$A_3 = \{(r, \varphi) | R_2 \leq r \leq R_3 = R_2 + t_2 \quad 0 \leq \varphi \leq \alpha\} \tag{23}$$

The thickness t_i $(i = 1, 2)$ are small in comparison with R_0. Following Arutyunjan and Abramyan [1] and Chabanjan [2] we assume that the stress function $U_i = U_i(r, \varphi)$ $(i = 1, 3)$ is a linear function of the radial coordinate r and satisfies the boundary conditions (10), (11), and the continuity conditions formulated by Eqs. (12) and (13). According to the above-mentioned requirements we have

$$U_1(r, \varphi) = \frac{U(R_1, \varphi)}{t_1} (r - R_0) \quad (r, \varphi) \in A_1 \tag{24}$$

$$U_2(r, \varphi) = -\frac{U(R_2, \varphi)}{t_2} (r - R_3) \quad (r, \varphi) \in A_3 \tag{25}$$

Here, we introduce the next designation $U_2(r, \varphi) = U(r, \varphi)$. Denote G_i $(i = 1, 3)$ the shear modulus of the thin isotropic elastic shell whose thickness is t_i $(i = 1, 2)$. The shear modulus in radial and tangential direction of cylindrically orthotropic cross section A_2 are represented by G_r and G_φ. From Eqs. (14) and (15) we obtain the next boundary conditions for $U = U(r, \varphi)$ [1,2]

$$U(R_1, \varphi) - \mu_1 \left. \frac{\partial U}{\partial r} \right|_{r=R_1} = 0 \quad 0 \leq \varphi \leq \alpha \tag{26}$$

$$U(R_2, \varphi) + \mu_2 \left. \frac{\partial U}{\partial r} \right|_{r=R_2} = 0 \quad 0 \leq \varphi \leq \alpha \tag{27}$$
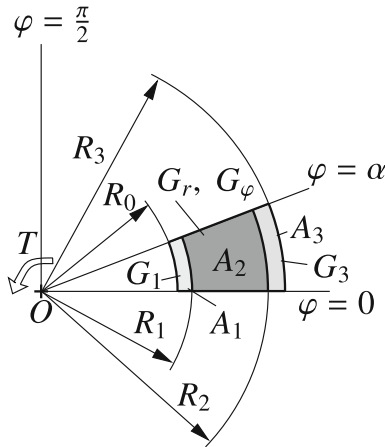
Fig. 2 Orthotropic cross section reinforced by thin shells

Here

$$\mu_1 = t_1 \frac{G_1}{G_\varphi}, \qquad \mu_2 = t_2 \frac{G_3}{G_\varphi} \qquad 0 \le \varphi \le \alpha \tag{28}$$

The solution of Saint-Venant's torsion of cylindrically orthotropic annular wedge-shaped bar strengthened by on its curved boundary surfaces by thin isotropic elastic shells is obtained from the next boundary value problem

$$\frac{\partial^2 U}{\partial r^2} + \frac{1}{r} \frac{\partial^2 U}{\partial r^2} + \frac{g^2}{r^2} \frac{\partial^2 U}{\partial \varphi^2} = -2G_\varphi \qquad g^2 = \frac{G_\varphi}{G_r} \ (r, \varphi) \in A_2 \tag{29}$$

$$U(r, 0) = U(r, \alpha) = 0 \qquad R_1 \le r \le R_2 \tag{30}$$

$$U(r, \varphi) - \mu_1 \frac{\partial U}{\partial r} = 0 \qquad r = R_1 \qquad 0 \le \varphi \le \alpha \tag{31}$$

$$U(r, \varphi) + \mu_2 \frac{\partial U}{\partial r} = 0 \qquad r = R_2 \qquad 0 \le \varphi \le \alpha. \tag{32}$$

We look for the solution of the boundary value problem formulated by Eqs. (29)–(32) in the next form

$$U(r, \varphi) = \sum_{k=1}^{\infty} u_k(r) \sin \lambda_k \varphi \qquad \lambda_k = (2k - 1) \frac{\pi}{\alpha} \tag{33}$$

It is evident $U = U(r, \varphi)$ satisfies the boundary conditions (30). In order to obtain the expression of $u_k = u_k(r)$ we will use the next Fourier's series representation of $-2G_\varphi$

$$-2G_\varphi = -\frac{8G_\varphi}{\alpha} \sum_{k=1}^{\infty} \frac{\sin \lambda_k \varphi}{\lambda_k} \tag{34}$$

Substitution of Eq. (33) into Eq. (29) we obtain

$$\frac{d^2 u_k}{dr^2} + \frac{1}{r} \frac{du_k}{dr} - \frac{p_k^2}{r^2} u_k = -\frac{8G_\varphi}{\alpha \lambda_k} \qquad p_k = g\lambda_k \quad (k = 1, 2, \dots) \tag{35}$$

The general solution of the ordinary differential equation (35) is as follows

$$u_k(r) = a_k r^{p_k} + b_k r^{-p_k} + c_k r^2 \qquad c_k = -\frac{8G_\varphi}{\alpha \lambda_k (4 - p_k^2)} \quad (k = 1, 2, \dots) \tag{36}$$

The constants a_k and b_k can be computed from the boundary conditions (31) and (32). A detailed computation gives

$$a_k = c_k \frac{h_{1k}}{h_k} \qquad b_k = -c_k \frac{h_{2k}}{h_k} \qquad (k = 1, 2, \dots) \tag{37}$$

$$
\begin{aligned}
h_k = {} & \mu_1 \mu_2 p_k^2 R_1^{2p_k} + \mu_2 p_k R_1^{2p_k+1} + \mu_1 p_k R_2 R_1^{2p_k} - R_2 R_1^{2p_k+1} \\
& + \mu_1 \mu_2 p_k^2 R_2^{2p_k} + \mu_2 p_k R_2^{2p_k} R_1 + \mu_1 p_k R_2^{2p_k+1} + R_2^{2p_k+1} R_1
\end{aligned}
\tag{38}
$$

$$
\begin{aligned}
h_{1k} = {} & -\mu_2 p_k R_1^{p_k+3} + R_2 R_1^{p_k+3} - 2\mu_1 R_2 R_1^{p_k+2} + 2\mu_1 \mu_2 p_k R_1^{p_k+2} - R_2^{p_k+3} R_1 \\
& - 2\mu_2 R_2^{p_k+2} R_1 - \mu_1 p_k R_2^{p_k+3} - 2\mu_1 \mu_2 p_k R_2^{k+2}
\end{aligned}
\tag{39}
$$

$$
\begin{aligned}
h_{2k} = {} & 2\mu_2 \mu_1 p_k R_2^{p_k+2} R_1^{2p_k} - 2\mu_2 R_2^{p_k+2} R_1^{2p_k+1} + \mu_1 p_k R_2^{p_k+3} R_1^{2p_k} - R_2^{p_k+3} R_1^{2p_k+1} \\
& - 2\mu_1 \mu_2 p_k R_2^{2p_k} R_1^{p_k+2} + \mu_2 p_k R_2^{2p_k} R_1^{p_k+3} - 2\mu_1 R_2^{2p_k+1} R_1^{p_k+1} + R_2^{2p_k+1} R_1^{p_k+3}
\end{aligned}
\tag{40}
$$

The determination of the torsional function of the cylindrically orthotropic cross section A_2 is based on the coupled system of partial differential equations (17) and (18). In this section we use the next designation $\omega_2 = \omega$. According to Eqs. (17) and (18) we have

$$\frac{\partial \omega}{\partial r} = \frac{1}{rG_r} \frac{\partial U}{\partial \varphi} \qquad \frac{\partial \omega}{\partial \varphi} = -\frac{r}{G_\varphi} \frac{\partial U}{\partial r} - r^2 \tag{41}$$

The solution of system of partial differential equation for $\omega = \omega(r, \varphi)$ is as follows

$$\omega(r, \varphi) = \sum_{k=1}^{\infty} \left(\frac{a_k}{g} r^{p_k} - \frac{b_k}{g} r^{-p_k} + \frac{c_k \lambda_k}{2} r^2 \right) \cos \lambda_k \varphi \tag{42}$$

This solution is vanishes on the axis of symmetry of the cross section A_2 ($\varphi = \alpha/2$). Since the size of thickness of shell-like cross-sectional component is very small we assume that $\omega_i = \omega_i(r, \varphi)$ ($i = 1, 3$) can be represented as

$$\omega_1(r, \varphi) = \omega(R_1, \varphi) \quad (r, \varphi) \in A_1 \qquad \omega_3(r, \varphi) = \omega(R_2, \varphi) \quad (r, \varphi) \in A_3 \tag{43}$$

The torsional rigidity of the compound cross section is obtained by the application of Eq. (20). A simple computation gives the next results for S

$$S = S_1 + S_2 + S_3 \tag{44}$$

where

$$
\begin{aligned}
S_1 = 2 \int_{R_0}^{R_1} \int_0^{\alpha} r U_1(r, \varphi) \, dr \, d\varphi \\
= \sum_{k=1}^{\infty} \frac{2t_1}{3\lambda_k} \left(a_k R_1^{p_k} + b_k R_1^{-p_k} + c_k R_1^2 \right) (3R_0 + 2t_1) \sin^2 \frac{\lambda_k \alpha}{2}
\end{aligned}
\tag{45}
$$

$$
\begin{aligned}
S_2 = 2 \int_{R_1}^{R_2} \int_0^{\alpha} r U_2(r, \varphi) \, dr \, d\varphi = 4 \sum_{k=1}^{\infty} \Bigg[a_k \frac{R_2^{p_k+2} - R_1^{p_k+2}}{\lambda_k (p_k + 2)} \\
+ b_k \frac{R_2^{-p_k+2} - R_1^{-p_k+2}}{\lambda_k (-p_k + 2)} + \frac{c_k}{4\lambda_k} \left(R_2^4 - R_1^4 \right) \Bigg] \sin^2 \frac{\lambda_k \alpha}{2}
\end{aligned}
\tag{46}
$$

$$
\begin{aligned}
S_3 = 2 \int_{R_2}^{R_3} \int_0^{\alpha} r U_3(r, \varphi) \, dr \, d\varphi \\
= \sum_{k=1}^{\infty} \frac{2t_2}{3\lambda_k} \left(a_k R_2^{p_k} + b_k R_2^{-p_k} + c_k R_2^2 \right) (3R_2 + 2t_2) \sin^2 \frac{\alpha \lambda_k}{2}
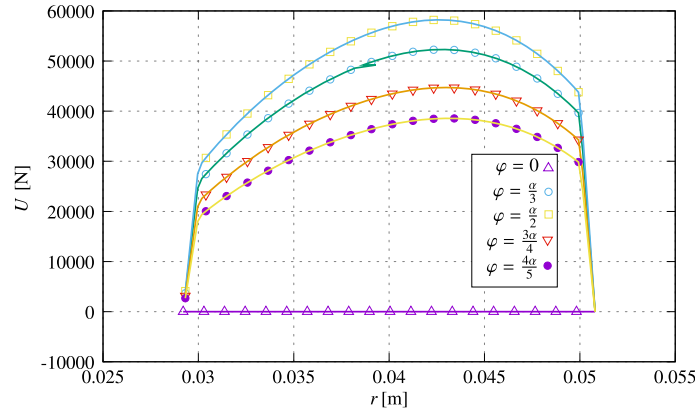\end{aligned}
\tag{47}
$$

Fig. 3 Prandtl's stress function as a function of radial coordinate
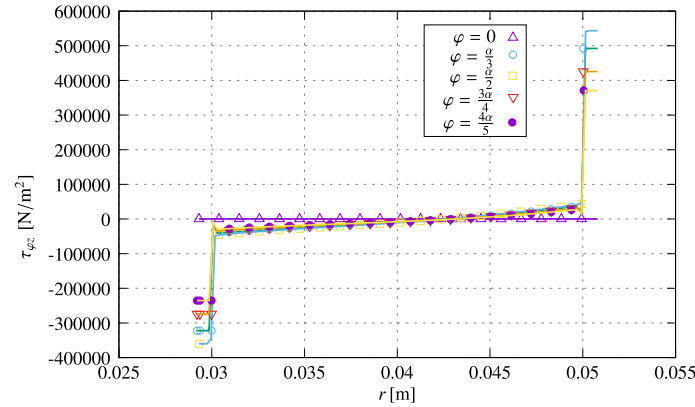

Fig. 4 Shearing stress $\tau_{\varphi z}$ for five different values of polar angle

The analytical solution of isotropic homogeneous elastic wedge-shaped bar which was given by Madhavi A and Madhavi Y [7] is recovered from the solution of Saint-Venant torsion problem presented in Sect. 3 of this paper if

$$R_0 = R_1, \quad R_2 = R_3, \quad G_1 = G_2 = 0, \quad \mu_1 = \mu_2 = 0, \quad G_r = G_\varphi = G. \tag{48}$$

4 Numerical example

The following data are used in the numerical example which illustrates the application of formulae of Sect. 3

$$R_1 = 0.03\,\text{m} \quad t_1 = 0.0008\,\text{m} \quad R_2 = 0.05\,\text{m} \quad t_2 = 0.0008\,\text{m} \quad \alpha = \frac{\pi}{4} \tag{49}$$

$$G_1 = 4.5 \times 10^9\,\text{Pa} \quad G_3 = 7.5 \times 10^9\,\text{Pa} \tag{50}$$

$$G_r = 3 \times 10^8\,\text{Pa} \quad G_\varphi = 6 \times 10^8\,\text{Pa} \quad \vartheta = 10^{-2}\,\text{rad/m} \tag{51}$$

The plots of the Prandtl's stress function as a function of radial coordinate for five different values of polar angle are shown in Fig. 3.

The plots of the shearing stress $\tau_{\varphi z}$ for five different values of polar angle against radial coordinate are presented in Fig. 4.

The illustration of the shearing stresses τ_{rz} as a function of radial coordinate for five different values of polar angle are given in Fig. 5.

The contour lines of the Prandtl's stress function are shown in Fig. 6.

The plots of the torsional function for five different values of polar angle against radial coordinate r are presented in Fig. 7.
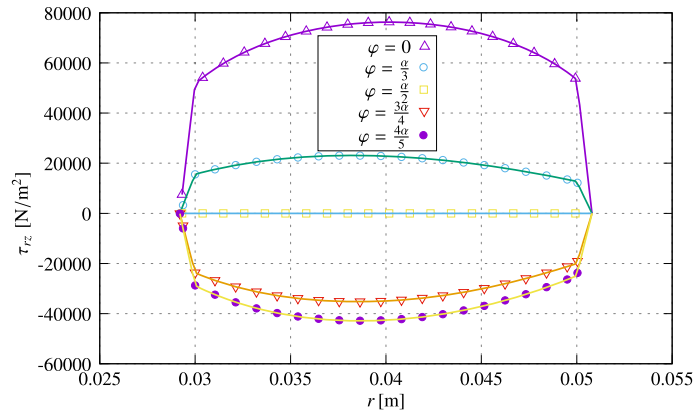
Fig. 5 Shearing stress τ_{rz} for five different values of polar angle
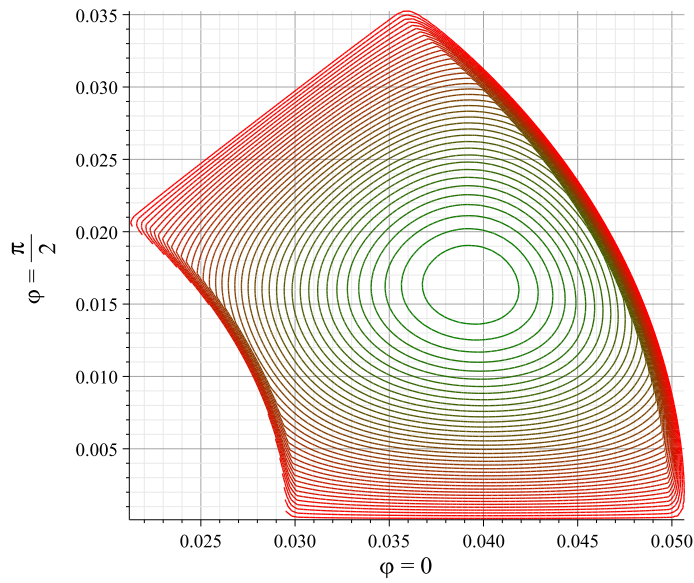

Fig. 6 Contour lines of Prandtl's stress function
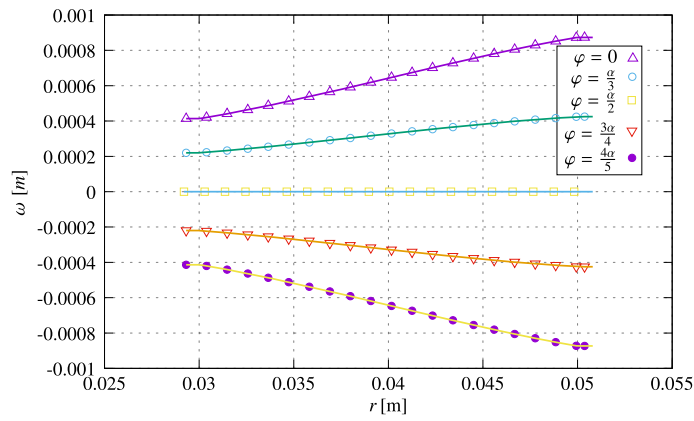

Fig. 7 Torsional function for five different values of polar angle
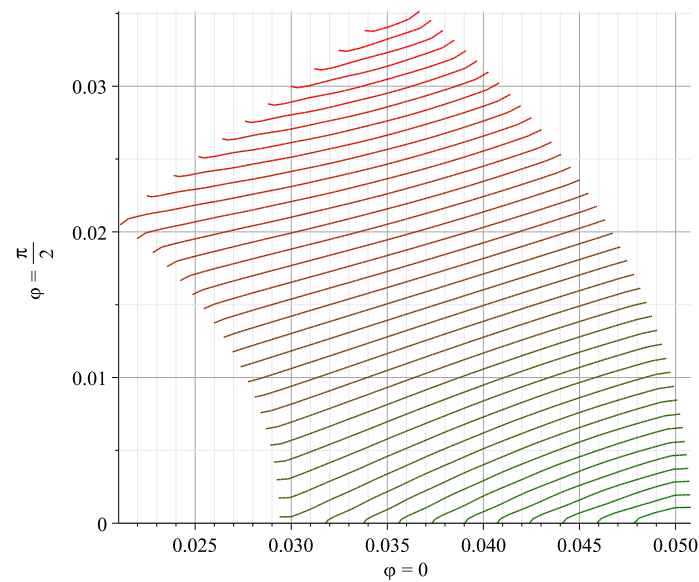
Fig. 8 Contour lines of the torsion function

Table 1 Comparison of approximate solution presented in this paper with the exact analytical results

$t = 0.0008$ m	
$S_1 = 0.580\,641\,224\,2\,\text{Nm}^2$	$S_1 = 0.580\,641\,534\,4\,\text{Nm}^2$
$S_2 = 52.119\,295\,730\,\text{Nm}^2$	$S_2 = 52.119\,287\,530\,\text{Nm}^2$
$S_3 = 1.254\,489\,661\,\text{Nm}^2$	$S_3 = 1.254\,461\,320\,\text{Nm}^2$
$S = 53.954\,426\,61\,\text{Nm}^2$	$S = 53.954\,390\,38\,\text{Nm}^2$
$V = 6.505\,579\,875 \times 10^4\,\text{N}$	$V = 6.505\,579\,700 \times 10^4\,\text{N}$
$t = 0.008$ m	
$S_1 = 50.124\,423\,18\,\text{Nm}^2$	$S_1 = 50.124\,423\,82\,\text{Nm}^2$
$S_2 = 34.793\,060\,94\,\text{Nm}^2$	$S_2 = 34.790\,606\,30\,\text{Nm}^2$
$S_3 = 81.627\,664\,\text{Nm}^2$	$S_3 = 81.627\,726\,\text{Nm}^2$
$S = 166.545\,149\,\text{Nm}^2$	$S = 166.545\,210\,\text{Nm}^2$
$V = 1.826\,756\,944 \times 10^5\,\text{N}$	$V = 1.826\,546\,927 \times 10^5\,\text{N}$
$t = 0.015$ m	
$S_1 = 104.029\,283\,2\,\text{Nm}^{42}$	$S_1 = 104.029\,280\,8\,\text{Nm}^2$
$S_2 = 16.757\,482\,98\,\text{Nm}^2$	$S_2 = 16.557\,478\,73\,\text{Nm}^2$
$S_3 = 220.061\,291\,\text{Nm}^2$	$S_3 = 220.061\,215\,\text{Nm}^2$
$S = 340.848\,057\,\text{Nm}^2$	$S = 340.647\,974\,\text{Nm}^2$
$V = 5.430\,432\,283 \times 10^5\,\text{N}$	$V = 5.430\,431\,167 \times 10^5\,\text{N}$

The contour lines of the torsion function are shown in Fig. 8. The torsional rigidity of the beam components B_1, B_2, B_3 and the whole compound cross section are as follows

$$S_1 = 0.3635213\,\text{Nm}^2 \quad S_3 = 0.9494349\,\text{Nm}^2 \quad S_2 = 43.47721\,\text{Nm}^2 \tag{52}$$

$$S = 44.79005\,\text{Nm}^2 \tag{53}$$

5 Comparison of approximate solution with exact analytical solution

Table 1 shows the effect of the thickness of outer and inner shell-layers to the accuracy of the solution given by this paper. The accuracy of the solution is measured by the torsional rigidities S_1, S_2 and S_3 of the cross-sectional components and a one value of Prandtl's stress function

$$V = U\left(\frac{R_1 + R_2}{2}, \frac{\alpha}{2}\right). \tag{54}$$

The first column of Table 1 are derived from the solution of boundary value problem formulated by Eqs. (29–32). The second column of Table 1 contains the results of exact analytical solutions of torsional problem which satisfy Eqs. (4–15).

The following data are used for calculation of the results for Table 1

$$R_0 = 0.035 \, \text{m} \quad R_3 = 0.055 \, \text{m} \quad t_1 = t_2 = t \quad \alpha = \frac{\pi}{4} \tag{55}$$

$$G_1 = 4.5 \times 10^9 \, \text{Pa} \quad G_3 = 7.5 \times 10^9 \, \text{Pa} \tag{56}$$

$$G_r = 3 \times 10^8 \, \text{Pa} \quad G_\varphi = 6 \times 10^8 \, \text{Pa} \tag{57}$$

6 Conclusion

In the present paper, the Saint-Venant torsion of the compound cylindrically orthotropic wedge-shaped bar has been studied. An analytical solution is given for the uniform torsion of the cylindrical orthotropic annular wedge shaped bar whose curved boundary segments are strengthened by thin isotropic elastic shells. The presented solution is valid for the vertex angle of compound cross section between 0 and 2π. Closed form formulae are derived for the Prandtl's stress function, torsion function, shearing stresses and torsional rigidity. Example illustrates the applications of the presented formulae.

Declarations

Conflict of interest On behalf of all authors, the corresponding author states that there is no conflict of interest.

References

1. Arutyunyan, N.H., Abramyan, B.L.: Torsion of Elastic Bodies. In Russian) Fizmatgiz, Moscow (1962)
2. Chobanjan, K.S.: Stresses in Compound Elastic Bodies. (In Russian) Izd. An. Apm. janslkoj SSSR, Erevan (1987)
3. Ecsedi, I., Baksa, A.: Saint-Venant torsion of cylindrical orthotropic elliptical cross section. Mech. Res. Commun. **99**, 42–46 (2019). https://doi.org/10.1016/j.mechrescom.2019.06.006
4. Ecsedi, I., Lengyel, A.J., Baksa, A.: Torsion of cylindrical orthotropic composite bar with cross section of a sector of solid circle. MultiScience XXXIII. In microCAD Int. Multidiscip. Conf. **D**(2–5), 1–9 (2019). https://doi.org/10.26649/musci.2019.038
5. Leknitskii, S.G.: Torsion of Anisotropic and Non-homogenous Beams. (in Russian) Izd. Nauka, Fiz-Mat. Literaturi, Moscow (1971)
6. Leknitskii, S.G.: Theory of Elasticity of an Anisotropic Body. MIR Publisher, Moscow (1981). https://doi.org/10.1107/S0365110X64002171
7. Madhavi, A., Madhavi, Y.: A novel analytical solution for warping analysis of annular wedge-shaped bars. Arch. Appl. Mech. **150**, 258 (2021). https://doi.org/10.1007/s00419-020-01858-1
8. Milne-Thomson, M.L.: Antiplane Elastic Systems. Springer, Berlin (1962). https://doi.org/10.1007/978-3-642-85627-3
9. Rand, O., Rovenski, W.: Analytical Methods in Anisotropic Elasticity. Birkhäser (2005). https://doi.org/10.1007/b138765
10. Sadd, H.M.: Elasticity. Theory, Application and Numerics. Elsevier, London (2005). https://doi.org/10.1016/B978-0-12-374446-3.X0001-6
11. Sarkisyan, V.S.: Some Problems of Anisotropic Elastic Bodies. Izd. Erevan University Press, Erevan (1970). In Russian
12. Sarkisyan, V.S.: Some Problems of Mathematical Theory of Elasticity of an Anisotropic Body. Izd. Erevan University Press, Erevan (1976). (**In Russian**)
13. Sokolnikoff, I.S.: Mathematical Theory of Elasticity. McGraw-Hill, Chennai (1956). https://doi.org/10.2307/3608899
14. Soós, E.: Sur le probléme de Saint-Venant dans le cas des barres hétérogénes avae anisotropic cylindrique. Bull. Math. de la Soc.Sci.Math.Phys. de la RPP **7**(55), 61–75 (1963)